MATEC Web of Conferences **6**, 01004 (2013)
DOI: 10.1051/matecconf/20130601004

Thermal stress estimation in relation to spalling of HSC restrained with steel rings at high temperatures

T. Tanibe[1], M. Ozawa[2], R. Kamata[1], R. Sato[3] and K. Rokugo[3]

[1] *Research & Development Laboratory, Taiheiyo Materials Corporation, Sakura City, Japan*
[2] *Division of Environmental Engineering Science, Gunma University, Kiryu City, Japan*
[3] *Department of Civil Engineering, Gifu University, Gifu City, Japan*

Abstract. This paper reports on an experimental study regarding the behavior of steel ring-restrained concrete in response to fire exposure. The study was conducted to enable estimation of thermal stress based on steel ring strain in such concrete under the conditions of a RABT 30 heating curve. The specimens used were made from high-strength concrete (Fc: 80 MPa) restrained using steel rings with thicknesses of 0.5, 8 and 18 mm.

1. INTRODUCTION

Fire represents one of the most severe risks to buildings and concrete structures because it often results in explosive concrete spalling stemming from two phenomena. The first is restrained thermal dilation resulting in biaxial compressive stress states parallel to the heated surface, which leads to tensile stress in the perpendicular direction [1]. The second is the build-up of concrete pore pressure due to vaporization of physically/chemically bound water resulting in tensile loading on the microstructure of the heated concrete [2]. Polypropylene fibers are often added to high-strength concrete (HSC) as an effective measure to prevent explosive spalling. A number of studies have also analytically demonstrated that the influence of thermal stress on explosive spalling is greater than that of vapor pressure [3–6]. However, few papers to date have outlined actual experimental studies on the exact influence of thermal stress [7]. The authors previously reported that a method involving the restraint of concrete with steel rings in heat testing can be used to clarify characteristics of thermal stress and explosive spalling behavior [8].

This paper reports on an experimental study regarding the behavior of steel ring-restrained concrete in response to fire exposure. The study was conducted to enable estimation of thermal stress based on steel ring strain in such concrete under the conditions of a RABT 30 heating curve. The high-strength concrete specimens (Fc: 80 MPa) used measured $\varphi 300 \times 100$ mm and were restrained using steel rings with thicknesses of 0.5, 8 and 18 mm.

2. THERMAL STRESS ESTIMATION

Figure 1 highlights the method adopted to estimate thermal stress. The specimens were made using concrete restrained with steel rings, and were subjected to heating tests with target measurements of internal concrete temperature, steel ring temperature, steel ring strain, internal vapor pressure, spalling time and spalling depth. Internal concrete deformation caused by heat-related thermal expansion and vapor pressure was restrained by the steel rings, and compressive stress was induced. Although such test setups have previously enabled qualitative evaluation, no simple procedure to routinely quantify

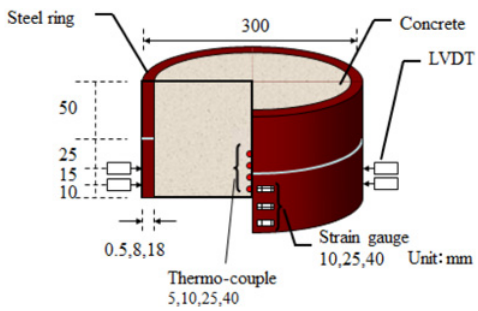

Figure 1. Specimen.

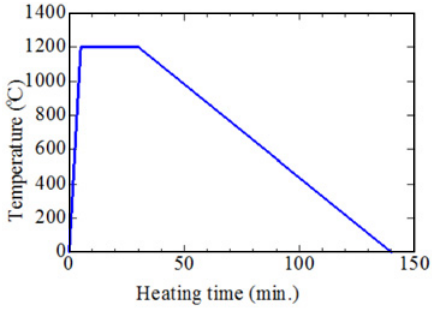

Figure 2. RABT 30 curve.

Table 1. Mix proportion of HSC (kg/m^3).

W/C	Water	Cement	Fine agg.	Coarse agg.1 (less 15 mm)	Coarse agg.2 (less 25 mm)	SP.
0.3	150	500	744	406	611	4

the characteristics of materials under restrained expansion has been established. In this study, an instrumented ring setup was used to quantify the behavior of concrete under restrained expansion during heating. Thermal stress calculation was based on the thin-walled cylinder model theory [9] as shown in Eqs. (1) and (2), and vapor pressure was measured at 10 and 20 mm from the heated surface.

$$\sigma_r = \varepsilon_t \times t \times E_s / R \tag{1}$$

$$\sigma_r = \sigma_{th} + \sigma_{vap}. \tag{2}$$

Here,
σ_r: restrained stress (MPa)
σ_{th}: thermal stress of concrete (MPa)
t: steel ring thickness (mm)
ε_t: steel ring strain
E_s: steel ring elastic modulus (MPa)
R: steel ring inside radius (mm)
σ_{vap}: vapor pressure (MPa).

3. EXPERIMENT OUTLINE

3.1 Concrete

Table 1 shows the mix proportions of the high-strength concrete (HSC) adopted for the experiment. A water-cement ratio of 0.3 and high-early-strength Portland cement (density: 3.15 g/cm^3) were used in this study, and crushed stone with a maximum grain size of 20 mm was added as coarse aggregate. The main component of the super-plasticizer (SP) was polymeric acid. After being cast, the concrete specimens were left in the formwork for one day, and were then wet cured at $20 \pm 2\,^{\circ}$C for two months. Heating tests for all specimens were performed after this time. Table 2 shows the values recorded for compressive strength, tensile strength, elastic modulus and water content ratio.

Table 2. Mechanical properties and water content ratio.

Compressive strength (MPa)	Elastic modulus (GPa)	Tensile strength (MPa)	Water content ratio (%)
84	42.9	6.1	4.1

Table 3. The specifications of the specimens.

No	Ring size mm			Concrete
	Thickness	Diameter of outside	Height	Outside of diameter
	mm	mm	mm	mm
300-0	0	300	/	284
300-0.5	0.5	300	50 mm*2	299
300-8	8	300	50 mm*2	284
300-18	18	300	50 mm*2	284

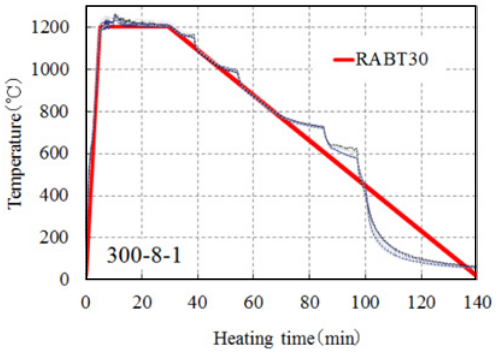

Figure 3. Temperatures inside the furnace.

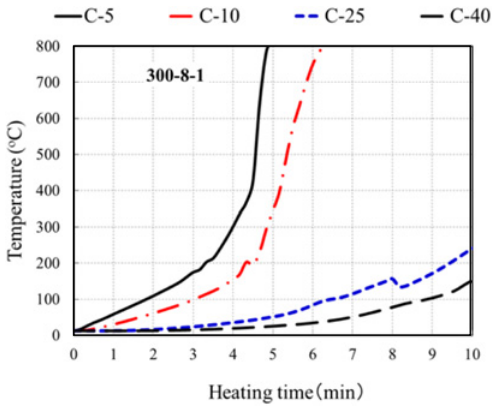

Figure 4. Concrete internal temperature.

3.2 Specimen dimensions and heating tests

Table 3 shows the specifications of the specimens. The steel rings used were 0.5, 8, and 18 mm thick, and a specimen with no steel ring was also tested. The configuration and dimensions of the specimens with steel rings are shown in Figure 1. Two pairs of rings were adopted (diameter: 300 mm; length: 50 mm; Ec (elastic modulus): 210 GPa; Fy (yield strength): 295 MPa). Three strain gauges, three thermocouples were attached 10, 25, 40 mm from the heated surface and outer surface of the steel rings. Two linear variable differential transformers (LVDTs; sensitivity: 1/1,000 mm) were also attached 10 and 25 mm from the heated surface and outer surface of the steel rings. Four type-K thermocouples were placed in the central zone of the specimens at 5, 10, 25 and 40 mm from the heated surface. The heating tests were based on a RABT 30 heating curve (Fig. 2). Strain gauges and thermocouples were attached at 10, 25, 40 mm from the heated surface.

4. STEEL RING THICKNESS/RESTRAINT RATIO

To estimate the restraint effect of using steel rings with various thicknesses, the restraint ratio was calculated using Equation (3).

$$I_r = (\Delta R_0 - \Delta R_n)/\Delta R_0. \tag{3}$$

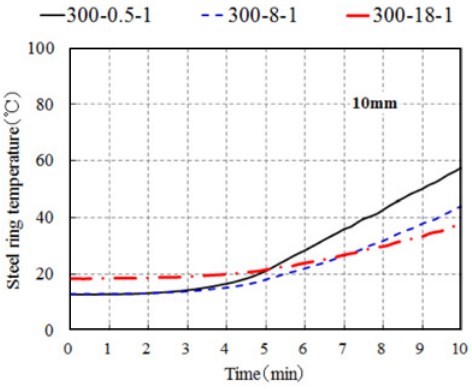

Figure 5. Steel ring temperature.

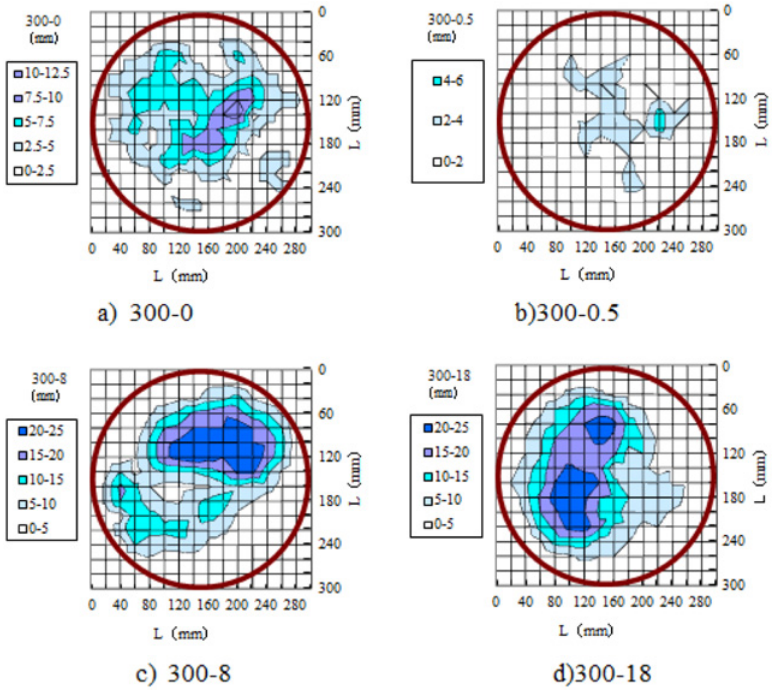

Figure 6. Depths of spalling.

Here,
I_r: restraint ratio
ΔR_0: diameter increment of free specimen during heating
ΔR_n: diameter increment of restrained specimen during heating
($n = 0.5, 8, 18$ mm).

The diameters were measured 10 and 25 mm from the heated surface using LVDTs, and the estimation times were 3, 5 and 10 minutes from the start of heating.

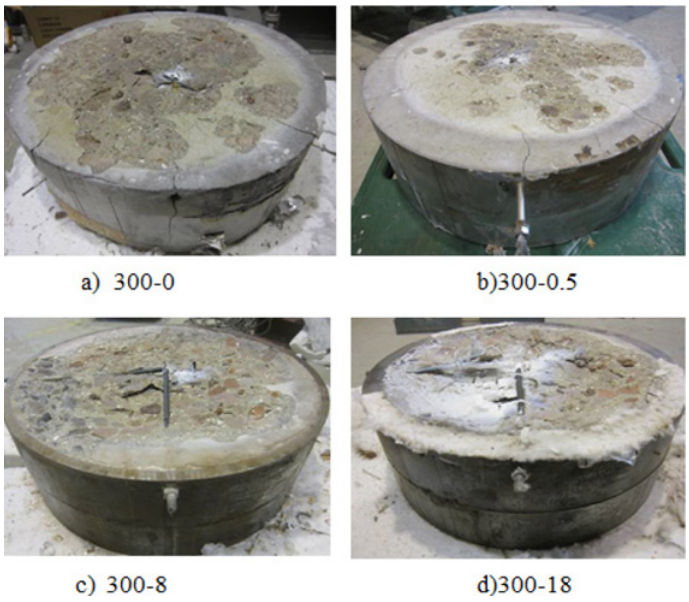

Photo 1. Damage to heated surfaces.

5. RESULTS AND DISCUSSION

5.1 Heating test

Figure 3 shows temperatures inside the furnace, and Figure 4 shows temperatures inside the specimens at 10 and 25 mm from the heated surface. The internal temperature changed drastically at 10 mm in the 300-8 and 300-18 specimens, which exhibited explosive spalling between 4 and 7 minutes. Meanwhile, the internal temperature in the 300-0 and 300-0.5 specimens changed gradually at 10 mm from the heated surface, indicating a low restraint effect. Figure 5 shows that the steel ring temperature was between 40 and 60 °C at 10 mm (the gauge point) from the heated surface at 10 minutes. It was considered that the strain gauge could be used at 10 minutes because its temperature limit is 80 °C.

5.2 Spalling depth

Figure 6 and Photo 1 show results for the depth of spalling and damage to heated surfaces for all specimens after the heating test. The maximum values for the 300-0, 300-0.5, 300-8 and 300-18 specimens were 11, 8, 24 and 26 mm, respectively. Accordingly, the restraint effect was considered large for the 300-8 and 300-18 specimens.

5.3 Thermal stress

Figure 7 shows the results of restrained stress calculation using the strain of the ring 10 mm from the heated surface for the 300-0.5, 300-8 and 300-18 specimens. After 10 minutes of heating, thermal stress levels reached 2.2, 7 and 9 MPa, respectively, at 10 mm. These results indicate that steel ring thickness is a dominant factor in thermal stress.

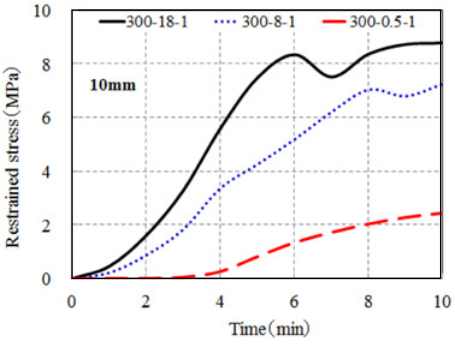

Figure 7. Restrained stress.

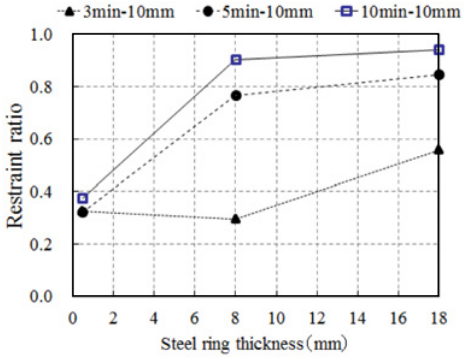

Figure 8. Restraint ration and steel ring thickness.

5.4 Restraint ratio

Figure 8 shows the restraint ratio and thickness of steel rings at 10 mm from the heated surface. The ratios were from 0.3 to 0.57 for the 300-0.5, 300-8 and 300-18 specimens, and were small before spalling at 3 minutes. Spalling started once the values reached 0.3, 0.8 and 0.85, respectively. The ratios were 0.3, 0.9 and 0.9, respectively, at 10 minutes. The restraint ratio of 0.9 (indicating almost full restraint) for the 300-8 and 300-18 specimens suggest that the ideal steel ring thickness is 8 mm.

6. CONCLUSIONS

The results obtained from the study can be summarized as follows:

1) In terms of spalling depth, the restraint effect was considered to be large for the 300-8 and 300-18 specimens.
2) After 10 minutes of heating, thermal stress levels were 2.2, 7 and 9 MPa for the 300-0.5, 300-8 and 300-18 specimens, respectively, at 10 mm from the heated surface. These results suggest that steel ring thickness is a dominant factor in thermal stress.
3) The restraint ratios were 0.3, 0.9 and 0.9 for the 300-0.5, 300-8 and 300-18 specimens, respectively, at 10 minutes. The ratio of 0.9 (indicating almost full restraint) for the latter two suggest that the ideal steel ring thickness is 8 mm.

This study was supported by Japan's Kajima Engineering Foundation 2011. The authors would like to express their gratitude to the organization for its financial support.

References

[1] Ulm, F. J., Coussy, O., Bazant, Z. P., The Chunnel Fire. II Analysis of concrete damage, *Journal of Engineering Mechanics*. 125, 1999, 283–289.
[2] Anderberg, Y., Spalling phenomena in HPC and OC, *Proceedings of the International Workshop on Fire Performance of High-Strength Concrete*, Phan, L. T., Carino, N. J., Duthinh, D., Garboczi, E. (eds.), Gaithersburg, MD: NIST; 1997, 69–73.
[3] Kalifa, P., Menneteau, F. D., Quenard, D., Spalling and pore pressure in HPC at high temperatures, *Cement and Concrete Research*, 30, 2000,1915–1927.

[4] Phan, L. T., Pore pressure and explosive spalling in concrete, *Materials and Structures*, 41, 2000, 1623–1632.
[5] Khoury, G. A., Willoughby, B., Polypropylene fibres in heated concrete Part 1: Molecular structure and materials behavior, *Magazine of Concrete Research*, 60, 2008, 125–136.
[6] Khoury, G. A., Polypropylene fibres in heated concrete Part 2: Pressure relief mechanisms and modelling criteria, *Magazine of Concrete Research*, 60, 2008, 189–204.
[7] Connolly, R. J., The Spalling of Concrete in Fires, *PhD thesis submitted to Aston University,* 1995.
[8] Tanibe, T. et al., Explosive spalling behavior of restrained concrete in the event of fire, *Proceedings of the 2nd International Rilem Workshop on Concrete Spalling due to Fire Exposure*, Koender, E. A., Dehn, F. (eds.) Netherlands, Delft, 2011, 319–326.
[9] Kogouchi, Y., Engineering of Ductwork, Mechanical Design, *Kougaku-tosho* (in Japanese), 1964.